MOLECULAR AND CELLULAR BIOLOGY, May 2004, p. 3782–3793 Vol. 24, No. 9
0270-7306/04/$08.00+0 DOI: 10.1128/MCB.24.9.3782–3793.2004

Normal Development and Fertility of Knockout Mice Lacking the Tumor Suppressor Gene *LRP1b* Suggest Functional Compensation by *LRP1*

Peter Marschang,[1]† Jochen Brich,[1]‡ Edwin J. Weeber,[2] J. David Sweatt,[2] John M. Shelton,[3] James A. Richardson,[4] Robert E. Hammer,[5] and Joachim Herz[1]*

Departments of Molecular Genetics,[1] Internal Medicine,[3] Pathology,[4] and Biochemistry,[5] University of Texas Southwestern Medical Center, Dallas, Texas 75390, and Division of Neuroscience, Baylor College of Medicine, Houston, Texas 77030[2]

Received 9 January 2004/Returned for modification 22 January 2004/Accepted 5 February 2004

LRP1b and the closely related LRP1 are large members of the low-density lipoprotein receptor family. At the protein level LRP1b is 55% identical to LRP1, a multifunctional and developmentally essential receptor with roles in cargo transport and cellular signaling. Somatic LRP1b mutations frequently occur in non-small cell lung cancer and urothelial cancers, suggesting a role in the modulation of cellular growth. In contrast to LRP1, LRP1b-deficient mice develop normally, most likely due to its restricted expression pattern and functional compensation by LRP1 or other receptors. LRP1b is expressed predominantly in the brain, and a differentially spliced form is present in the adrenal gland and in the testis. Despite the presence of a potential furin cleavage site and in contrast to LRP1, immunoblotting for LRP1b reveals the presence of a single 600-kDa polypeptide species. Using a yeast two-hybrid approach, we have identified two intracellular proteins, the postsynaptic density protein 95 and the aryl hydrocarbon receptor-interacting protein, that bind to the intracellular domain of LRP1b. In addition, we have found several potential ligands that bind to the extracellular domain. Analysis of LRP1b knockout mice may provide further insights into the role of LRP1b as a tumor suppressor and into the mechanisms of cancer development.

The low-density lipoprotein (LDL) receptor family comprises seven closely related receptors in mammals. These receptors share a typical arrangement of ligand-binding domains, epidermal growth factor homology domains, and YWTD propeller domains in their extracellular part and contain a cytoplasmic tail with at least one NPXY motif. Two LDL receptor family members, i.e., the LDL receptor and the LDL receptor-related protein 1 (LRP1) are widely expressed in nearly all cells, while the pattern of the other members (very low density lipoprotein [VLDL] receptor, apoER2, and megalin) is more restricted. The biological functions of the receptors are highly diverse and include the uptake of lipoproteins and other ligands, the regulation of cell surface proteinase activity, the regulation of Ca^{2+} homeostasis, and important functions in brain development and neurotransmission. Besides their classical role in receptor-mediated endocytosis, evidence is now accumulating that many of the family members play important roles in signal transduction through adaptor molecules that bind to their cytoplasmic tails (8).

Two very large receptors of the LDL receptor family have been well characterized. LRP1 contains 31 ligand-binding repeats and binds a variety of ligands, including apoE-carrying lipoproteins, α2-macroglobulin, and proteinases and their inhibitors. A unique feature of LRP1 is the fact that this receptor is cleaved by furin in a late secretory compartment, which results in a carboxyl-terminal 85-kDa fragment and a noncovalently linked 515-kDa subunit. LRP1 can bind numerous ligands and has been implicated in a variety of biological functions, including lipoprotein metabolism, the regulation of the activity of proteinases and lysosomal enzymes, and neurotransmission. In addition, LRP1 is used as a receptor by certain viruses and toxins (13). Megalin, the largest member of the family, is expressed on the apical surface of polarized epithelia in the kidney, lung, intestine, brain, and other organs as a single-chain 600-kDa receptor. It plays an important role in Ca^{2+} homeostasis by mediating the reuptake of 25 (OH)-vitamin D_3 and by binding and internalizing parathyroid hormone in the kidney (20). To uncover the biological function of these receptors, knockout models have been generated. Mice homozygous for a disruption in the LRP1 gene die early during embryonic development, indicating a critical role of LRP1 in development (9). Most megalin knockout mice die perinatally from respiratory insufficiency and show holoprosencephaly as well as structural abnormalities of the lungs and kidneys (33).

LRP1b, originally termed LRP-DIT (short for "LRP-deleted in tumors"), is a recently discovered member of the LDL receptor family. The unusually large LRP1b gene spans approximately 500 kb on the long arm of chromosome 2 (2q21.2), a region that frequently shows allelic loss in advanced tumors of different origin. In the first report by Liu et al., the authors found homozygous deletions or abnormal transcripts of the LRP1b gene in nearly 50% of the non-small cell lung cancer cell lines studied (19). Similarly, alterations of the LRP1b gene have been described in high-grade urothelial cancer (17). LRP1b is therefore considered as a candidate tumor suppres-

* Corresponding author. Mailing address: Department of Molecular Genetics, 5323 Harry Hines Blvd., Dallas, TX 75390. Phone: (214) 648-5633. Fax: (214) 648-8804. E-mail: Joachim.Herz@UTSouthwestern.edu.

† Present address: Department of Internal Medicine, University of Innsbruck, Innsbruck, Austria.

‡ Present address: Zentrum für Neurowissenschaften, Universität Freiburg, 79104 Freiburg, Germany.

sor gene. The LRP1b gene codes for a type I transmembrane glycoprotein of 4,599 amino acids, which corresponds to a calculated molecular mass of approximately 500 kDa in the absence of glycosylation. It comprises 32 ligand-binding repeats that are arranged in four regions. Among the LDL receptor family, it shows the highest degree of identity to LRP1 (55% identity of the amino acid sequence). LRP1b has a nearly identical overall structure compared to LRP1, with the exception of two additional exons, of which one (exon 68) codes for an additional repeat in the fourth ligand-binding repeat cluster and another (exon 90) encodes a 33-amino-acid sequence within the cytoplasmic tail that shows no homology to other known proteins.

The human and mouse sequences of LRP1b are highly conserved, with 86% identical residues. In the first report of LRP1b, a broad distribution in human tissues was reported (19). However, in a subsequent publication the receptor was found to be almost exclusively expressed in the brain (18). Using a minireceptor containing the carboxyl-terminal part of the molecule including the fourth ligand-binding repeat region, Liu et al. showed that some of the well-known ligands of LRP1, namely, the receptor-associated protein (RAP), urokinase plasminogen activator, tissue-type plasminogen activator, and plasminogen activator inhibitor type 1 also bind to this LRP1b construct (18).

Here we describe the generation of LRP1b knockout mice. These animals show no obvious phenotype, probably due to functional compensation by other LDL receptor family members. We have investigated the tissue distribution of the full-length receptor and of a splice variant lacking exon 90 in the mouse and show that LRP1b is expressed on the cell surface as single-chain receptor. Furthermore, we have identified two intracellular adaptor proteins, as well as several potential extracellular ligands that suggest diverse physiological functions for LRP1b.

MATERIALS AND METHODS

Animals, cell culture, and antibodies. Mice were held according to institutional guidelines with free access to food (6% mouse or rat diet 7002; Harlan Teklad, Madison, Wis.) and water on a cycle of 12 h of dark, 12 h of light. Human embryonal kidney (HEK) 293 cells (ATCC CRL-1573) and 293 S cells (kindly provided by J. Nathan, John Hopkins University, Baltimore, Md.) were cultured in Dulbecco's modified Eagle's medium (Cellgro; Mediatech Inc., Herndon, Va.) containing 10% fetal calf serum (Atlanta Biologicals, Norcross, Ga.), and 100 IU of penicillin/ml and 100 μg of streptomycin/ml (both from Mediatech Inc.) in an 8% CO_2 humidified atmosphere at 37°C. To produce a polyclonal antiserum against LRP1b, a peptide corresponding to the 13 carboxyl-terminal amino acids of LRP1b with an additional cysteine residue at the amino terminus (NH_2-C PKKIEIGIRETVA-COOH) was synthesized. The peptide was coupled to maleimide-activated keyhole limpet hemocyanin (Imject; Pierce, Rockford, Ill.) via the amino-terminal cysteine, and the conjugate was used to immunize rabbits. The antiserum was purified by Thiophilic adsorption chromatography (Clontech, Palo Alto, Calif.) followed by affinity purification on a column coated with the peptide used for immunization. Polyclonal antibodies against the carboxyl terminus of LRP1 and the VLDL receptor as well as purified rat megalin have been described previously (6, 11, 33). A monoclonal antibody against the FLAG epitope (M2) was purchased from Sigma-Aldrich (St. Louis, Mo.).

Generation of LRP1b-deficient mice. Two fragments of genomic mouse DNA were amplified using the LA PCR kit from Takara (Panvera, Madison, Wis.). The short arm (0.9 kb) corresponding to the major part of intron 88 was amplified using primers 5′-AATT**CTCGAG**TGTATGTAGTCTAATGAAAC TAACAGTGG-3′ and 5′-AATT**CTCGAG**CTCCATTGATGATAGGCTGC CTTCTAATTG-3′ (restriction sites used for cloning are shown in boldface). The long arm (9.8 kb) was amplified from intron 87 using the primers 5′-AATT**GCGGCCGC**CAAAGAGCAGCAAATCTGAGCATATCAG-3′ and 5′-AATT**GCGGCCGC**CCTGTTGGGATGGTTGGTTAGATAACTTTTG-3′. The two fragments were cloned into the targeting vector on either site of the *pol2sneobpA* expression cassette. The vector also contained two copies of the herpes simplex virus thymidine kinase gene at the 3′ end of the short arm. After linearization, the targeting vector was introduced into mouse 129SvEv embryonal stem cells grown on STO feeder cells via electroporation and selected with G418 (Invitrogen, Carlsbad, Calif.) and ganciclovir (Sigma) as described previously (32). Homologous recombination was assessed by PCR, and positive clones were injected into C57BL/6 blastocytes. The resulting male chimeras were bred with C57BL/6 females, and a total of nine heterozygous agouti pups were obtained and bred to homozygosity. Except where indicated otherwise, all experiments were performed with these LRP1b$^{-/-}$ mice on a mixed C57BL/6 × 129SvEv background. Mice were genotyped by PCR using the downstream primer 5′-TACTTCCACTTCTTGGAAGATAAAGGAAA T-3′ combined with the upstream primer 5′-CATCGTGCCACTTGTCCTTTTGG TGACC-3′ for the wild-type allele and upstream primer 5′-GATTGGGAAGACA ATAGCAGGCATGC-3′ for the disrupted allele, respectively. For the detection of the genotypes by Southern blotting, a probe was amplified from genomic DNA using primers 5′-AATT**AAGCTT**AAGAGAAAAAGAAGAACAAAGACAATTAGAA GG-3′ and 5′-AATT**AAGCTT**GTAAGATTAGTCCTAATGAAATGGAC-3′. This 900-bp fragment comprises exon 89 and parts of intron 89 of the LRP1b gene. After subcloning into pCR2.1-TOPO (Invitrogen) the fragment was cut out with HindIII and radiolabeled with [^{32}P]dCTP using the random primer labeling method. Tail DNA of the mice was digested with BamHI and BglII, transferred to Hybond XL membranes (Amersham Biosciences, Piscataway, N.J.), and then subjected to Southern hybridization at 42°C using Ultrahyb buffer (Ambion, Austin, Tex.) according to the instructions of the manufacturer.

To obtain LRP1b$^{-/-}$ mice on an inbred 129SvEv background, male chimeras were bred with 129SvEv females. The offspring was screened for heterozygotes by PCR genotyping and then bred to homozygosity. Identical results were obtained on the mixed and inbred backgrounds.

Preparation of crude membrane fractions and immunoblotting. Wild-type and LRP1b$^{-/-}$ mice were anesthetized with halothane, and tissues were harvested, cut into pieces, and immediately put into prechilled 20 mM Tris (pH 8.0)–150 mM NaCl–1 mM $CaCl_2$ containing EDTA-free Complete proteinase inhibitors (Roche, Indianapolis, Ind.). After homogenization with a polytron homogenizer (Brinkmann/Kinematika, Westbury, N.Y.) and two low-speed spins (1,500 × *g* and 10,000 × *g*), the homogenate was centrifuged at 100,000 × *g* for 30 min at 4°C to separate the membrane fraction (pellet) from the soluble fraction (cytosol). The pellet was resuspended in 50 mM Tris (pH 8.0)–80 mM NaCl–2 mM $CaCl_2$ with EDTA-free Complete proteinase inhibitors. Triton X-100 was then added to both the membrane and cytosolic fractions to a final concentration of 1%. The membrane fraction was passed several times through a 28-gauge needle and cleared by a second centrifugation at 100,000 × *g* to remove insoluble material. Total protein concentrations were determined with the DC protein assay from Bio-Rad (Hercules, Calif.). Equal amounts of total protein were separated by sodium dodecyl sulfate polyacrylamide electrophoresis (SDS-PAGE) under reducing conditions and transferred to nitrocellulose membranes (C-Hybond; Amersham) using 18 mM Tris–150 mM glycine with 0.01% SDS as a transfer buffer. Transfer efficiency and equal loading was verified by staining with Ponceau S (Sigma). Western blotting was performed using 5% nonfat milk as blocking agent and horseradish peroxidase-labeled anti-rabbit or anti-mouse antibodies (Amersham) followed by enhanced chemiluminescence detection (Supersignal West Pico; Pierce). Where indicated, membrane fractions or whole-cell lysates were digested with endoglycosidase H_f (1,000 U), neuraminidase (50 U), or peptide N glycosidase F (PNGase F) (500 U) (all from New England Biolabs, Beverly, Mass.). Digestions were carried out overnight at room temperature in the presence of 10 μM leupeptin (Calbiochem, San Diego, Calif.) and 200 μM phenylmethylsulfonyl fluoride (Sigma) followed by SDS-PAGE as described above.

Hippocampal slice preparation and CA1 electrophysiology. Hippocampal slices were prepared from the brains of wild-type mice, LRP1b$^{-/-}$ mice, RAP$^{-/-}$ mice, and double-knockout (LRP1b$^{-/-}$; RAP$^{-/-}$) mice as described previously (30). Extracellular field recordings were obtained from the area CA1 stratum radiatum. Stimulation was supplied with a bipolar Teflon-coated, platinum electrode and recording was obtained with the use of a glass microelectrode (resistance, 1 to 4 mΩ). Tetani used to evoke CA1 long-term potentiation (LTP) consisted of two trains of 100-Hz stimulation for 1 s, with each train separated by a 20-s interval. Stimulus intensities were adjusted to give population excitatory postsynaptic potentials with slopes that were ≤50% that of maximum determined from an input-output curve. Experimental results were obtained only from those slices that exhibited stable baseline synaptic transmission for a minimum of 30 min before the LTP-inducing stimulus was given. Slices from wild-type and

knockout animals were used in side-by-side experiments in order to reduce the variability of day-to-day changes in recordings. Data from paired-pulse facilitation (PPF) and LTP experiments were analyzed using a two-way analysis of variance, with posthoc tests performed using the method of Bonferroni.

RNA preparation and RT-PCR. Wild-type mice were anesthetized with halothane, and tissues were removed and immediately snap-frozen in liquid nitrogen. After addition of RNA-Stat 60 (Tel-Test, Friendswood, Tex.), the tissues were homogenized with a Polytron homogenizer and total RNA was prepared according to the instructions of the manufacturer. Reverse transcriptase PCR (RT-PCR) was performed from 1 μg of total RNA using the Titanium One step RT-PCR kit or by first-strand cDNA synthesis with Power Script followed by PCR with Advantage 2 (all from Clontech). The primers used to amplify the whole LRP1b cytoplasmic tail were primer P1 5′-AATT**GAATTC**AAGAGAAA AAGAAGAACAAAGACAATTAGAAGG-3′ and primer P2 5′-AATT**GGAT CC**TTATGCTACTGTTTCTCTGATGCCAATTTC-3′, exons 90 and 91 were amplified using primer P3 5′-TTTT**GAATTC**TCCAGGTACATAGGGGGAGG GTCCAGTGCTTTC-3′ and primer P2.

Control reactions were carried out using primers specific for mouse β-actin (Clontech). Bands amplified with LRP1b-specific primers were cut out and confirmed by DNA sequencing.

In situ hybridization. The cytoplasmic tail of LRP1b (400 bp) was amplified using primers P1 and P2 and TA cloned into pCR2.1-TOPO (Invitrogen) in both orientations to generate an antisense probe and a sense control. The C-terminal parts of the coding sequences of postsynaptic density protein 95 (PSD-95) (600 bp) and aryl hydrocarbon receptor (AhR)-interacting protein (AIP) (500 bp) were cut out from the library clones using BamHI and XhoI or PstI and XhoI, respectively. The fragments were then cloned into pBluescript SK and KS vectors to yield the antisense probes and sense controls. Riboprobes were transcribed in the presence of ^{35}S-UTP (Amersham) using the T7 promoter with the Maxiscript kit (Ambion) and purified by column chromatography using NucAway spin columns (Ambion) or mini Quick Spin RNA columns (Roche). In situ hybridization was performed on sagittal brain sections from adult wild-type mice as described elsewhere (7, 25).

Cloning and expression of LRP1b constructs. Two different membrane-spanning LRP1b minireceptors were constructed. To generate an untagged region IV LRP1b minireceptor, the leader peptide sequence of human LRP1b was amplified from human brain cDNA (Marathon-ready; Clontech) using primers 5′-A ATT**CTCGAG**ACAATGTCCGAGTTTCTCCTCGCCTTACTCAC-3′ and 5′-AATT**GCCGGC**GGCTCCCACGGTCAGCACCCT-3′. Amino acids 3275 to 4599 of LRP1b, comprising the fourth ligand-binding domain region, the transmembrane region, and the cytoplasmic tail of LRP1b. were amplified from human brain cDNA using the primers 5′-AATT**GCCGGC**CTCTGCATGATA AATAATGGTGGTTGCA-3′ and 5′-AATT**GGTACC**TTATGCCACTGTCTC TCTTATACCAATTTC-3′ (primer P4) by long-range PCR (Advantage 2). Both fragments were cloned into pcDNA3.1myc/HIS (Invitrogen) after digestion with XhoI and NgoMIV or NgoMIV and KpnI, respectively. The resulting LRP1b minireceptor contains two additional amino acid residues (alanine-glycine, encoded by the introduced cloning site **GCCGGC**) between the signal sequence and region IV of LRP1b. Due to a stop codon at the 3′ end of the insert, the myc and His tags are not expressed. No other sequence alterations were introduced. To generate a LRP1b minireceptor with an amino-terminal FLAG tag, amplification was performed using primer P4 and the upstream primer 5′-AA**AGATCT**GCT CTGCATGATAAATAATGGTGGTTGCA-3′. After digestion with BglII and KpnI, the fragment was cloned into p3xFLAG-CMV-9 (Sigma), which contains the preprotryspin leader sequence followed by three FLAG epitopes upstream of the multiple cloning site. Soluble LRP1b ectodomains comprising the ligand-binding domain regions I, II, III, and IV as well as the adjacent epidermal growth factor precursor homology repeats and one YWTD propeller were amplified by PCR and cloned into p3xFLAG-CMV-9 to add three N-terminal FLAG epitopes. The following primers were used to amplify the sequences from mouse brain cDNA: ectodomain I (corresponding to amino acids 31 to 517), 5′-AA**G CGGCCGC**GTTGTGTGACCCTGGCGAATTTCTTT-3′ and 5′-AATT**GGAT CC**TTATTTGCATGACCTGCCATCGCT-3′; ectodomain II (corresponding to amino acids 844 to 1570), 5′-AA**GCGGCCGC**GATCTGTAAACCTGGAGAA TTTCGCTG-3′ and 5′-AA**AGATCT**TTAATAGCAGGTTTTCTTGTCAGAG GAAAGCTT-3′; ectodomain III (corresponding to amino acids 2509 to 3314), 5′-AA**GCGGCCGC**GTCTTGTAATATCTATTCTGAGTTTGAGTGTGG A-3′ and 5′-AA**AGATCT**TTATAAGCAAGTTCTATTATCAGCTGCAAGGT AGA-3′; ectodomain IV (corresponding to amino acids 3316 to 4208), 5′-AA**G CGGCCGC**GAACTGCACAGCCAGTCAGTTTCGA-3′ and 5′-AATT**GGATC C**TTAATGGCAGGTCCCATTCATCATATATTT-3′. The amplified ectodomains were cloned into p3xFLAG-CMV-9 using the NotI and BamHI or NotI and BglII sites, respectively. All constructs were verified by sequencing with an automated DNA sequencer (ABI Prism 3100 Genetic Analyzer; Applied Biosytems, Foster City, Calif.). LRP1 minireceptors of region II and region IV have been described previously (35). For the expression of membrane-spanning minireceptors, HEK 293 cells were transfected with 2.5 μg of plasmid DNA per 60-mm-diameter dish using Fugene 6 (Roche) according to the protocol supplied by the manufacturer. After 48 h, the cells were washed with phosphate-buffered saline and lysed in phosphate-buffered saline containing 0.5% Triton X-100 and protease inhibitors (EDTA-free Complete). To express soluble LRP1b ectodomains; 5 μg of plasmid DNA per 60-mm-diameter dish was transfected into HEK 293 cells using the $Ca_3(PO_4)_2$ method (MBS-kit; Stratagene, La Jolla, Calif.). Transfections were carried out according to the instructions of the manufacturer with the exception that the transfection cocktail was left on the cells for 5 h and then replaced with serum-free Dulbecco's modified Eagle medium containing 0.2% bovine serum albumin (low endotoxin, immunoglobulin G free; Sigma). After 48 h, the supernatant was harvested and centrifuged at 5,000 × *g* for 20 min.

Yeast two-hybrid screen. The cytoplasmic tail of LRP1b was amplified from a mouse brain cDNA library (Clontech) using primers P1 and P2. This PCR yielded two amplification products corresponding to the full-length LRP1b tail (400 bp) and an alternatively spliced tail lacking exon 90 (LRP1bΔ90, 300 bp). Both fragments were cloned into pLexA (Clontech) and verified by sequencing. A third bait vector containing exon 90 only was constructed by cloning the amplification product of primers P3 and 5′-AATT**GGATCC**CTACCCAAAAG TTAGTGGTCCTTTCAAATCAGA-3′. The bait vectors were used to screen a mouse brain cDNA library as previously described (7). DNA from positive clones was transformed into KC8 *Escherichia coli* cells (Clontech) by electroporation, and colonies containing the library plasmids were selected on agar plates containing M9 minimal medium without tryptophan. Candidate proteins were identified by sequencing and confirmed by retransformation into EGY48 [p8op-lacZ] as well as by a yeast-mating assay after transformation into the YM4271 strain.

GST pulldown. Glutathione *S*-transferase (GST) fusion proteins were constructed by cloning the sequences of the library clones directly into pGEX-4T1 (Amersham) via the EcoRI and XhoI site. For PSD-95, individual domains were amplified from a plasmid containing the full-length rat PSD-95 cDNA (kindly provided by Thomas C. Südhof, UT Southwestern Medical Center, Dallas, Tex.) and cloned into pGEX-KG (10). The primers used for amplification were as follows: PDZ domain 1, 5′-GTTG**GAATTC**CCATGGAGTATGAGGAGATCA CATTGG-3′ and 5′-GTTG**AAGCTT**TCAGAGTTTGATCTCCATGACCTTTT CGG-3′; PDZ domain 2, 5′-GTTG**GAATTC**CAGCCGAAAAGGTCATGGAG ATCAAAC-3′ and 5′-GTTG**AAGCTT**TCAGTCTGGGGGAGCATAGCTGT CACTC-3′; PDZ domain 3, 5′-GGTTG**GAATTC**GGGAACCAAGGCGGATC GTGATCC-3′ and 5′-GTTG**AAGCTT**TCAATGGATCTTGGCCTCGAATCG AC-3′; SH3 domain, 5′-GGTTG**GAATTC**CCAAGAGGGGCTTCTACATTAG GG-3′ and 5′-GTTG**AAGCTT**TCACCTTGACCACTCTCGTCGCTCGACC-3′; guanylate-kinase-like (GK) domain, 5′-GTTG**GAATTC**CCTATGAGACGG TGACCCAGATGGAAG-3′ and 5′-GTTG**AAGCTT**TCACCAGATGTAGGG GCCTGAGAGGTC-3′. GST-RAP has been described previously (10). GST fusion proteins were expressed in BL-21 cells (Stratagene) after induction with isopropyl-thio-D-galactopyranoside (Invitrogen) and purified on glutathione-agarose (Sigma). The GST pulldown assays were performed as described elsewhere (7).

Affinity purification. For large-scale expression of secreted LRP1b ectodomains, HEK 293S (23) cells were transfected with the respective plasmids coding for LRP1b ectodomains I to IV. After selection with G418, stable clones were obtained for cells expressing ectodomains II, III, and IV. No stably producing clones could be obtained for ectodomain I. The correct expression and export of the ectodomains was proven by Western blotting of the culture supernatants. Stably transfected cells were expanded, trypsinized, and transferred to suspension cultures using spinner flasks (2 liters for ectodomain II, 1 liter for ectodomain III, and 1.5 liters for ectodomain IV) in serum-free IS-GRO medium (Irvine Scientific, Santa Ana, Calif.). After 96 h, the cultures were centrifuged twice at 5,000 × *g* and the supernatants were collected and concentrated using Millipore YM30 ultrafiltration membranes (Millipore, Billerica, Mass.). To immobilize the ectodomains, the concentrated supernatants were incubated with M2 anti-FLAG agarose (Sigma) in batch format for 6 h at 4°C. Crude membrane and soluble cytosolic fractions were prepared from the brains of 12 wild-type mice as described above with the exception that no Triton X-100 was added to the soluble cytosolic fraction in order to minimize the addition of detergent. Membrane fractions were combined with the soluble cytoplasmic fractions and incubated with the immobilized ectodomains in batch format overnight at 4°C. As a control, bacterial alkaline phosphatase (BAP) containing three N-terminal FLAG epitopes (Sigma) was bound to M2 anti-FLAG agarose and incubated the same way with brain tissue. On the next day, the beads were washed 3 times with

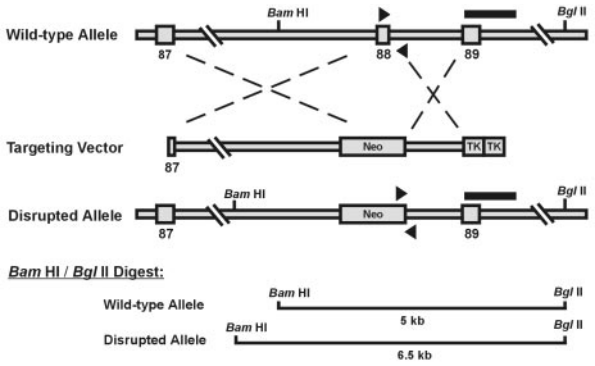

FIG. 1. Knockout strategy for the targeted inactivation of the LRP1b gene in the mouse. A targeting vector was constructed to replace exon 88 of the LRP1b gene, which codes for the membrane-spanning segment, with a neo cassette. Exons are symbolized as numbered rectangles. The position of the primers used for genotyping by PCR is indicated by arrowheads. The black horizontal bar indicates the location of the probe used for Southern blotting. The expected sizes of the bands for the wild-type and disrupted allele after digestion with BamHI and BglII are shown.

50 ml of 10 mM Tris (pH 7.5)–150 mM NaCl–2 mM $CaCl_2$ (TBS-Ca^{2+}). The agarose was then poured into columns and eluted with 3xFLAG peptide (100 μg/ml) in TBS-Ca^{2+}. Fractions containing protein were pooled, concentrated with Centricon 30 microconcentrators (Millipore), and then separated by 4-to-15% gradient SDS-PAGE. The gels were stained with colloidal Coomassie or by silver staining (Silver Quest, both from Invitrogen). Bands were cut out and proteins bound to LRP1b ectodomains were identified by reversed-phase nano-HPLC–ion-trap mass spectroscopy.

RESULTS

LRP1b $^{-/-}$ mice are phenotypically normal. Mice lacking the LRP1b gene in the germ line were generated using targeted homologous recombination by replacing the transmembrane exon 88 with a neomycin resistance cassette (Fig. 1). The disruption of the LRP1b gene was detected by allele-specific PCR (Fig. 2A). The wild-type specific band of 500 bp is only present in wild-type mice and heterozygotes, whereas the 300-bp fragment is specific for the knockout allele. We confirmed the disruption of the LRP1b gene by Southern blotting, where the wild-type specific band at 5 kb is replaced by a 6.5-kb band in LRP1b$^{-/-}$ mice (Fig. 2B). The absence of LRP1b protein in LRP1b$^{-/-}$ mice was proven by Western blotting of brain membrane preparations with a polyclonal antibody directed against the cytoplasmic tail of the receptor. Only in brains from wild-type mice, a 600-kDa band is seen with the anti-LRP1b antibody. As a control, the same samples were blotted with an LRP1 antibody resulting in equally strong bands at 600 kDa in all lanes. (Fig. 2C).

LRP1b$^{-/-}$ mice obtained on a mixed C57BL/6 129SvEv background (n = 190) appeared normal and were fertile with normal litter sizes. No abnormalities were observed over their entire life span, with the oldest animals close to 2 years of age. In all assays performed including brain histology, cholesterol level in plasma, and fasting triglycerides, they were indistinguishable from wild-type mice (data not shown). A total of 26 LRP1b$^{-/-}$ mice between 3 weeks and 12 months of age were sacrificed, and autopsies were performed. No tumors were detected in any of the animals. This suggests that the role of LRP1b as a tumor suppressor gene is conditional upon preceding events on the road to malignant transformation and that loss of LRP1b alone is not sufficient. In addition, LRP1b$^{-/-}$ mice were also generated on an inbred 129SvEv background (n = 9). These mice were also phenotypically normal. To test whether the homologous LRP1 molecule might functionally replace LRP1b in the knockout animals, LRP1b$^{-/-}$ mice were bred with mice deficient in RAP (31). RAP$^{-/-}$ mice show a reduced expression of LRP1 to approximately 20% compared to wild-type mice and were chosen as a model for reduced LRP1 expression, since complete LRP1 deficiency is embryonically lethal (9). However, these LRP1b$^{-/-}$; RAP$^{-/-}$ mice also did not show any obvious abnormalities.

Electrophysiology of LRP1b mutants. To test whether the absence of LRP1b might alter hippocampal synaptic transmission or plasticity we performed electrophysiologic characterizations of the well-defined Schaffer collateral synapses in area CA1. As shown in Fig. 3A, baseline synaptic transmission at Schaffer collateral synapses was not affected in mice lacking LRP1b and/or RAP compared to wild-type animals (wild type, n = 17; LRP1b$^{-/-}$, n = 17, RAP$^{-/-}$, n = 9; and LRP1b$^{-/-}$; and RAP$^{-/-}$, n = 20). To test for short-term synaptic plasticity, we examined PPF. PPF is a facilitation of neurotransmitter release likely due to residual calcium present in the presynaptic terminal following depolarization (36).

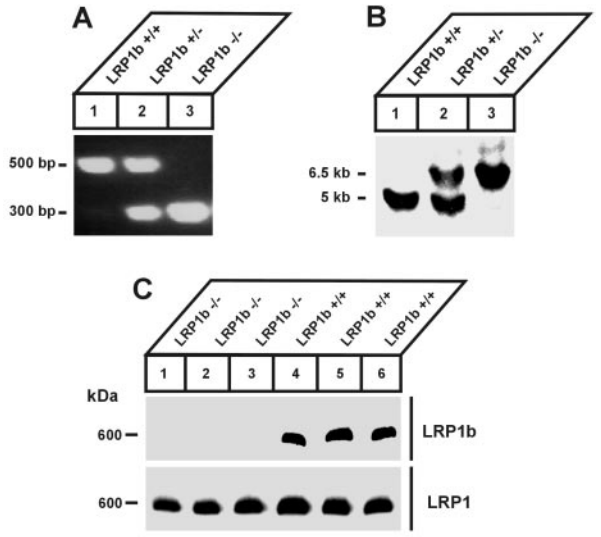

FIG. 2. Genotyping and absence of LRP1b protein expression in LRP1b$^{-/-}$ mice. (A) Genomic DNA was prepared from the tails of wild-type mice (lane 1) and mice heterozygous (lane 2) and homozygous (lane 3) for the disruption of the LRP1b gene. The DNA was amplified by PCR with allele-specific primers to detect the wild-type LRP1b allele (500 bp) and disrupted allele (300 bp), respectively. (B) Genomic DNA from the tails of mice with the genotypes indicated was digested with BamHI and BglII and separated on a 0.6% agarose gel. Southern blotting was performed with a ^{32}P-labeled probe 3′ of the short arm homology region. The size of the bands is shown (5-kb wild-type allele, 6.5-kb disrupted allele). (C) Crude membrane fractions were prepared from the brains of three homozygous LRP1b$^{-/-}$ mice (lanes 1 to 3) and three wild-type controls (lanes 4 to 6). Equal amounts of total protein (100 μg) were separated by SDS–4% PAGE, transferred to nitrocellulose membranes and subjected to Western blotting using antibodies against the carboxyl terminus of LRP1b (upper panel) and LRP1 (lower panel).

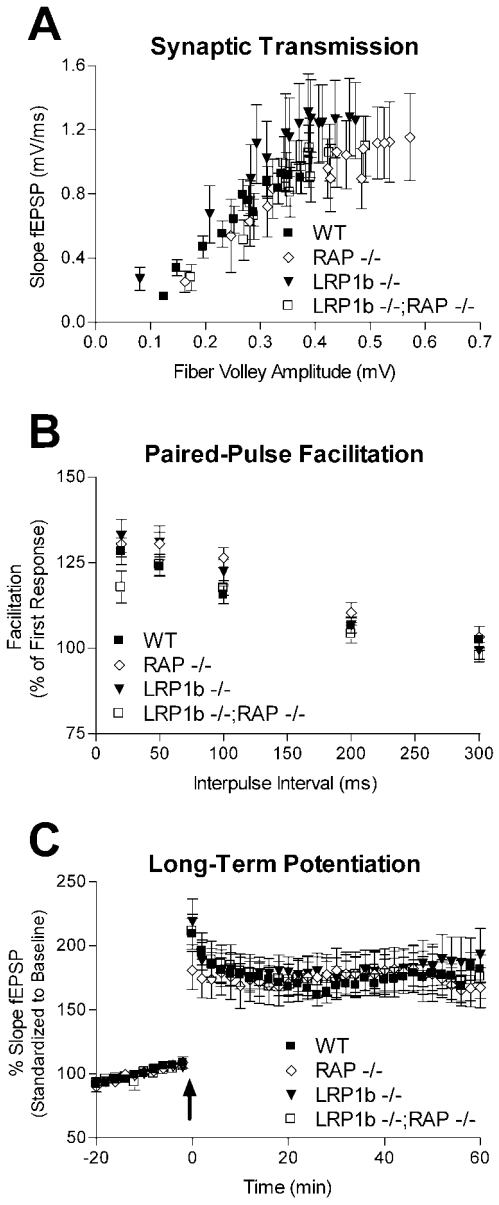

FIG. 3. Synaptic transmission and plasticity in mice lacking LRP1b and/or RAP. Hippocampal slices were prepared from the brains of wild-type (WT) mice, $RAP^{-/-}$ mice, $LRP1b^{-/-}$ mice, and $LRP1b^{-/-}$; $RAP^{-/-}$ double knockout mice. Baseline synaptic transmission represented as the slope of the field excitatory postsynaptic potential (fEPSP) compared to fiber volley amplitude at increasing stimulus intensities (A); PPF at IPI of 20, 50, 100, 200, and 300 ms (B); and LTP induced with two trains of 100-Hz stimulation for 1 s separated with a 20-s interval (indicated by an arrow) (C) are shown for each genotype. Data are shown as means ± standard errors of the means (error bars).

Moreover, PPF is a short-lived form of plasticity likely to be involved in some forms of learning and memory (27). The percent of PPF was determined at interpulse intervals (IPI) of 20, 50, 100, 200, or 300 ms (wild type, $n = 17$; $LRP1b^{-/-}$, $n = 17$; $RAP^{-/-}$, $n = 9$; and $LRP1b^{-/-}$; $RAP^{-/-}$, $n = 20$). Although a slight difference was seen at an IPI of 20 ms in the double $LRP1b^{-/-}$; $RAP^{-/-}$ mice, there was no significant difference in overall PPF in any of the animal groups tested (Fig. 3B). Hippocampal LTP is a use-dependent increase in synaptic efficacy believed to be similar to processes underlying long-term memory formation in mammals. We observed no differences in the induction or maintenance of LTP (wild type, $n = 14$; $LRP1b^{-/-}$, $n = 14$; $RAP^{-/-}$, $n = 9$; and $LRP1b^{-/-}$; $RAP^{-/-}$, $n = 17$) (Fig. 3C).

LRP1b is expressed in brain, adrenal gland, and testis. To reveal the physiological sites of LRP1b expression in the mouse, RT-PCR was performed using gene-specific primers within the cytoplasmic tail of the receptor. As shown in Fig. 4A, an LRP1b-specific amplification product could only be detected in RNA derived from brain (two bands of 400 and 300 bp), adrenal gland (one band at 300 bp), and testis (one band at 300 bp). The weak band in RNA from heart tissue is most likely nonspecific, since it could not be confirmed by DNA sequencing. In all other tissues examined, including liver, lung, kidney, muscle, adipose tissue, and the digestive tract, no amplification products were observed. To confirm these findings, we probed Western blots loaded with crude membrane preparations from different tissues of wild-type mice with an affinity purified polyclonal LRP1b antibody as shown in Fig. 4B. In brain tissue, a single band at approximately 600 kDa was observed, whereas in all other tissues tested, including testis and heart, no bands were visible. We could not obtain enough tissue from mouse adrenal glands to prepare membrane fractions.

To further localize the regions expressing LRP1b in the

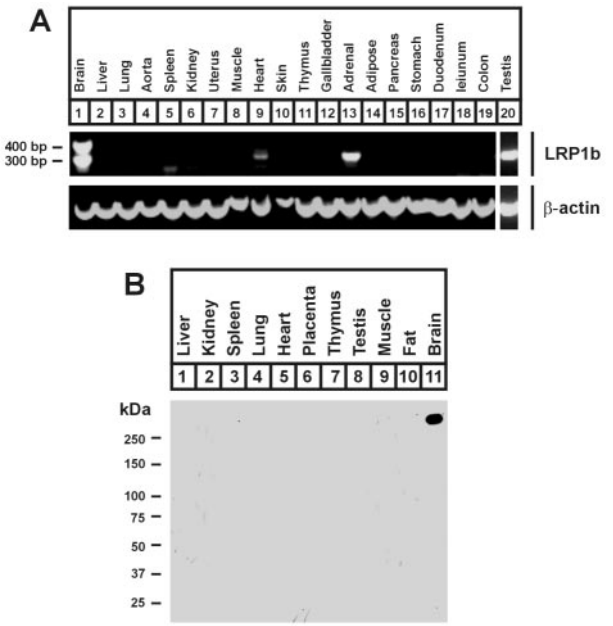

FIG. 4. Tissue distribution of LRP1b in the mouse. (A) Total RNA was isolated from murine tissues and amplified by RT-PCR using primers specific for the cytoplasmic tail of LRP1b. The size of the observed fragments (400 and 300 bp) is indicated. RNA integrity was ascertained by control amplifications with primers specific for mouse β-actin. (B) Crude membrane preparations of different mouse tissues were prepared from wild-type mice. Total protein (100 μg per lane) was separated by SDS-PAGE (4 to 15% acrylamide), transferred to nitrocellulose membranes and subjected to Western blotting using the affinity-purified LRP1b antibody.

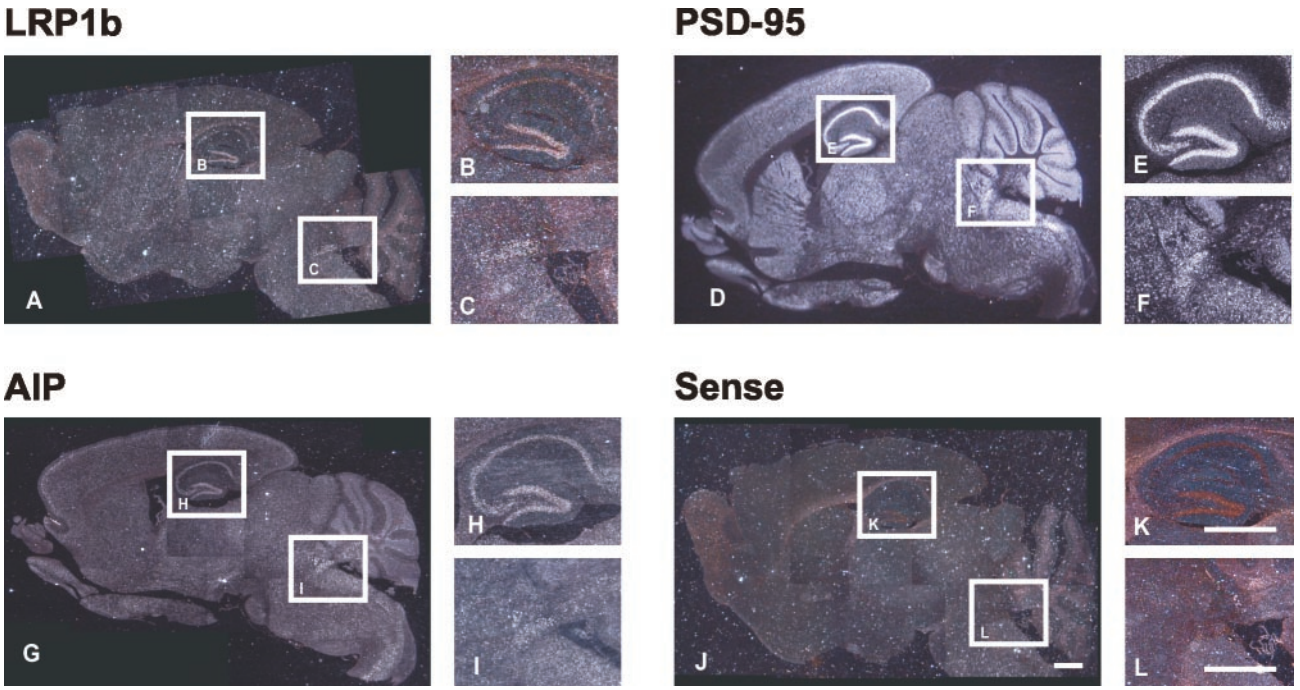

FIG. 5. Localization of LRP1b expression in the brain. Sagittal brain sections from adult wild-type mice were hybridized with antisense probes specific for LRP1b (A to C), PSD-95 (D to F), and AIP (G to I) as well as a sense control probe (J to L) by in situ hybridization. For each probe, a 1.6× objective magnification of the total brain as well as 4× objective magnifications of the hippocampus and the region around the fourth ventricle are shown. Scale bar, 1 mm.

brain we performed in situ hybridization on brain sections of adult wild-type mice. As shown in Fig. 5A to C, LRP1b expression is highest in the dentate gyrus of the hippocampus and in a region ventral of the fourth ventricle. No LRP1b mRNA could be detected in the testis by this technique, and the hybridization in the adrenal gland could not be evaluated due to high background of the sense probe in this tissue (data not shown).

An alternatively spliced form of LRP1b lacking exon 90. During the cloning of the cytoplasmic tail of LRP1b from a mouse brain cDNA library as well as from first-strand mouse brain cDNA, it became apparent that the cytoplasmic tail of LRP1b is present in two differentially spliced forms. To further investigate this alternative-splicing event, RT-PCR was performed using two primer pairs as shown in Fig. 6. Consistent with the results shown in Fig. 4A, two amplification products were observed in mRNA derived from mouse brain using primers P1 and P2. The 400-bp band corresponds to the full-length receptor tail, whereas the 300-bp band is derived from an alternatively spliced receptor lacking exon 90. Adrenal gland and testis appear to contain only transcripts with the shorter 300-bp tail. The identity of the respective bands was confirmed by DNA sequencing. The second primer pair (P3 and P2) amplifies exons 90 and 91 only. With this PCR, only RNA derived from brain gave a positive result (single band at 240 bp), whereas the other tissues (adrenal, testis, and liver) were negative, indicating that the splicing event that adds additional 33 amino acids to the intracellular domain of LRP1b is brain-specific.

LRP1b is not cleaved by furin. LRP1 is known to be cleaved by the proteinase furin in a trans-Golgi compartment and is

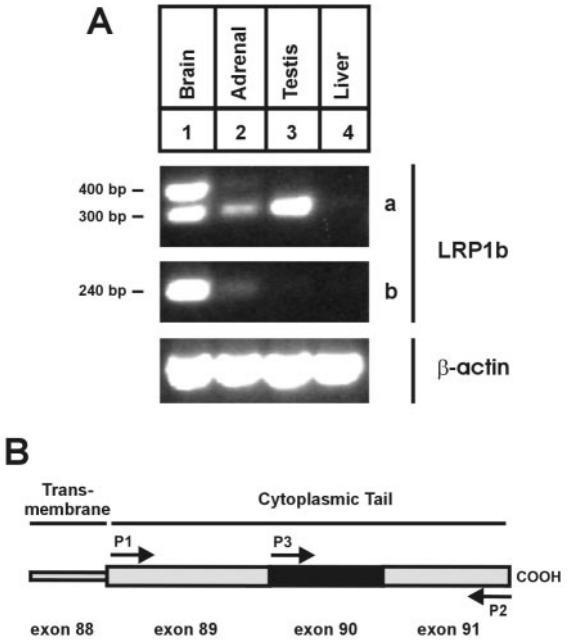

FIG. 6. Tissue specific alternative splicing of the cytoplasmic LRP1b tail. (A) Total RNA from mouse brain, adrenal gland, testis, and liver was transcribed by reverse transcriptase and subsequently amplified by PCR using primers P1 and P2 (upper panel, a), primers P3 and P2 (middle panel, b), or by primers specific for β-actin as a control (lower panel). The size of the amplification products with the LRP1b specific primers is shown. (B) The location of primers P1, P2, and P3 within the cytoplasmic tail of LRP1b is shown.

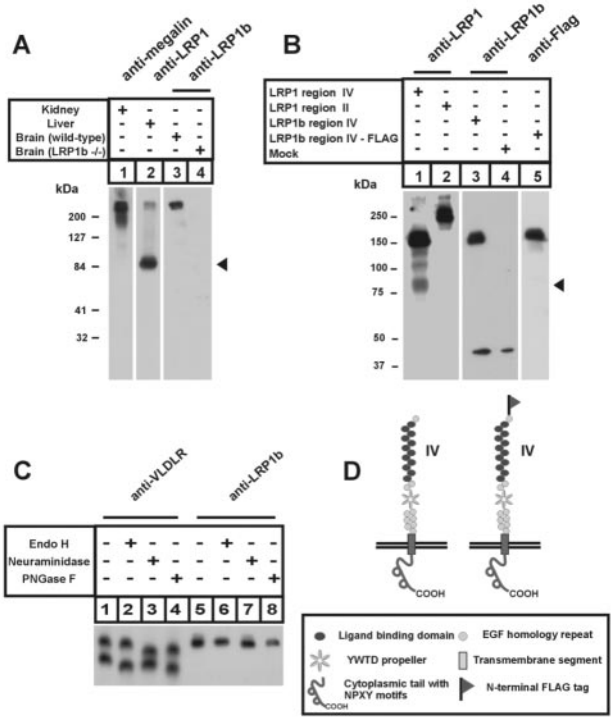

FIG. 7. LRP1b is not processed by furin. (A) Crude membrane preparations from mouse kidney (10 μg, lane 1), liver (50 μg, lane 2) and brain (100 μg, lane 3 wild-type, lane 4 LRP1b$^{-/-}$) were separated by SDS-PAGE (4 to 15% acrylamide) and subjected to Western blotting with antibodies against megalin (lane 1), LRP1 (lane 2) and LRP1b (lanes 3 and 4). The arrowhead indicates the expected position of a carboxyl-terminal fragment after furin cleavage, which is prominent in the case of LRP1 but missing in the other two receptors. (B) HEK 293 cells were transfected with membrane-bound minireceptors containing ligand-binding domain region IV of LRP1 (lane 1), region II of LRP1 (lane 2), region IV of LRP1b (lane 3), and region IV of LRP1b with an N-terminal FLAG tag (lane 5). Lane 4 is a control from mock-transfected cells. Equal amounts of lysates from these cells were separated by PAGE (4 to 15% acrylamide) followed by Western blotting with antibodies against the carboxyl terminus of LRP1 (lane 1 and 2), LRP1b (Lane 3 and 4), or against the FLAG epitope (lane 5). The arrowhead indicates the position of an expected carboxyl-terminal fragment after furin processing, which is only seen in cells transfected with the region IV LRP1 minireceptor. (C) Crude membrane preparations from mouse heart (lanes 1 to 4) or lysates from HEK 293 cells transfected with the LRP1b minireceptor were left untreated (lanes 1 and 5), or treated with endoglycosidase H (lanes 2 and 6), neuraminidase (lanes 3, and 7), or PNGase F (lanes 4 and 8). After overnight incubation, SDS–6% PAGE was performed followed by Western blotting using the anti-VLDL receptor (lanes 1 to 4) and anti-LRP1b (lanes 5 to 8) antibodies, respectively. (D) The structure of the LRP1b minireceptor with and without the amino-terminal FLAG tag is shown.

therefore present on the cell surface in the form of two noncovalently linked protein chains of 515 and 85 kDa (34). In a recent report, a similar cleavage event was described for an LRP1b minireceptor containing the fourth ligand-binding domain region (18). Since we had consistently seen only a single band on Western blots probed with our anti-LRP1b antibody, we performed additional experiments to detect possible cleavage products of LRP1b.

Figure 7A shows immunoblots of the three large members of the LDL receptor family. In liver membranes, Western blotting with an antibody against the carboxyl terminus of LRP1 showed a prominent band at 85 kDa and a weaker high-molecular-weight band. Conversely, in the Western blots of megalin and LRP1b from kidney and brain membranes, respectively, no additional bands at 85 kDa were seen. Identical results were obtained with lysates of HEK 293 cells transfected with LRP1 and LRP1b minireceptors. Only in cells transfected with an LRP1 minireceptor containing the ligand-binding domain region IV, an 85-kDa band corresponding to the furin-cleaved form was seen (Fig. 7B). This band is absent in HEK 293 cells transfected with a region II LRP1 minireceptor, which does not contain the furin cleavage site. In contrast to LRP1, we observed a band at approximately 160 kDa corresponding to the uncleaved protein, but the predicted 85-kDa band was never detected in HEK 293 cells transfected with an LRP1b minireceptor containing the putative furin cleavage site. The band at approximately 40 kDa is nonspecific, since it is also present in mock-transfected cells.

Similarly, in cells transfected with an analogous LRP1b minireceptor construct containing an amino-terminal FLAG tag, only a single band at approximately 160 kDa was observed. To prove the correct transport of the LRP1b minireceptor to the cell membrane, we performed glycosidase digests as shown in Fig. 7C. The VLDL receptor, which is known to be present as a mature receptor (upper band) and a precursor (lower band) served as a control. Digestion with endoglycosidase H, which cleaves immature high-mannose carbohydrates, results in a faster migration of the precursor form on SDS-PAGE. Neuraminidase cleaves terminal sialic acid residues from the mature receptor only, whereas PNGase F cleaves all N-linked carbohydrates. Similarly to the mature VLDL receptor, digestion of the LRP1b minireceptor with neuraminidase and PNGase F, but not endoglycosidase H, resulted in a shift in the apparent molecular weight. Thus, the mature LRP1b minireceptor has passed through the trans-Golgi compartment en route to the cell surface.

PSD-95 and AIP bind to the cytoplasmic tail of LRP1b. To identify intracellular proteins binding to the cytoplasmic tail of LRP1b, we performed a yeast two-hybrid screen using the LRP1b tail fused to the DNA-binding LexA protein as bait. A bait vector construct containing the full-length LRP1b tail (LRP1b), one containing the alternatively spliced tail lacking exon 90 (LRP1bΔ90), and a third one containing exon 90 only (LRP1bexon90) were constructed. The bait vector containing the full-length LRP1b tail showed weak autoactivation in the yeast two-hybrid system. Therefore, the screen of a mouse brain cDNA library was performed with the bait vector containing the alternatively spiced tail and identified positive clones were then tested against all three constructs in a yeast-mating assay. Table 1 shows the identity of the three library clones that we identified in this screen. All three candidate proteins were confirmed by retransformation and yeast mating and all three proteins bound both to the alternatively spliced as well as to the full-length LRP1b tail, but not to the bait protein containing exon 90 only. PSD-95 is a scaffolding protein that binds to several proteins in the postsynaptic density, including the LDL receptor family members LRP1, megalin, and ApoER2 (7). It contains three PDZ domains, one SH3 domain, and a GK domain (Fig. 8A). AIP (also referred to as ARA9 and XAP2) is an intracellular adaptor protein that binds to the AhR. It contains three tetratrico peptide repeats

TABLE 1. Intracellular proteins that interact with the cytoplasmic tail of LRP1b[a]

Protein	No. of clones	Insert size	Expression	Yeast mating	GST pulldown	Domain
PSD-95	3	1,400	Brain	LRP1b, LRP1bΔ90	Positive	PDZ1, PDZ3
AIP	1	1,200	Ubiquitous	LRP1b, LRP1bΔ90	Positive	TPR (?)
18.5 kDa	3	1,000		LRP1b, LRP1bΔ90	Negative	

[a] Intracellular proteins identified in the yeast two-hybrid screen are listed with the number of clones identified and the size of the insert in the prey vectors. The results of the confirmation assays (bait vectors giving a positive result in the yeast-mating assay, GST pulldown) are also shown. None of the proteins bound to the third bait vector (LRP1bexon90). For PSD-95, two domains (PDZ domains 1 and 3) were identified as mediating the binding of LRP1b in the GST pulldown. For AIP, the TPR domain responsible for binding has not been identified yet.

(TPR). A third, uncharacterized putative 18.5-kDa protein was identified that does not contain previously described protein interaction motifs (accession number GI 12837887). To confirm the binding to the LRP1b tail, a GST pulldown assay was performed using the isolated clones of AIP, the 18.5-kDa protein as well as the individual domains of PSD-95 as GST fusion proteins. As shown in Fig. 8B, the binding of LRP1b from brain membranes to AIP and PSD-95 (PDZ domains 1 and 3) could be confirmed. No binding was observed with PDZ domain 2, the SH3 domain and the GK domain of PSD-95, the 18.5-kDa protein or with GST alone. To support these observations, we tested whether AIP and PSD-95 are expressed in the same brain areas as LRP1b. As shown by in situ hybridization, both AIP and PSD-95 are widely expressed in the mouse brain and the expression pattern overlaps with that of LRP1b (Fig. 5D-I).

Identification of potential extracellular ligands of LRP1b. To screen for extracellular ligands of LRP1b, we constructed soluble secreted ectodomains corresponding to ligand-binding domain regions I, II, III, and IV of LRP1b. After transfection into HEK 293 cells, the ectodomains were detected via their N-terminal FLAG tag in the supernatant of transfected cells (Fig. 9A). Ectodomain II appeared as two bands on the SDS gels, presumably due to different glycosylation. To prove that the ectodomains are folded correctly and able to bind ligands, we performed GST pulldown assays with RAP, a known ligand of LRP1b family members. In this assay, ectodomains II and IV bound strongly, and ectodomain III weakly to RAP. In contrast, no binding to RAP was observed in the case of ectodomain I. With the exception of ectodomain IV, which bound weakly to GST, no binding was observed in the control experiments with GST.

For large-scale production of LRP1b ectodomains, suspension-adapted 293S cells were used. These experiments were performed for ectodomains II, III, and IV only, since no clones with consistent secretion of ectodomain I could be obtained from either 239 or 293S cells. Figure 10 shows the result of the affinity purification using immobilized ectodomains and mouse brain lysates. Most bands corresponding to bound proteins were eluted from the columns bearing ectodomain II and IV with the FLAG peptide. In the control lane (BAP), only a single band with the apparent molecular weight of BAP was present. The potential extracellular ligands of LRP1b identified by this approach are summarized in Table 2. Except for gpr69a and the laminin receptor precusor, at least two peptides were identified for each of the potential ligands.

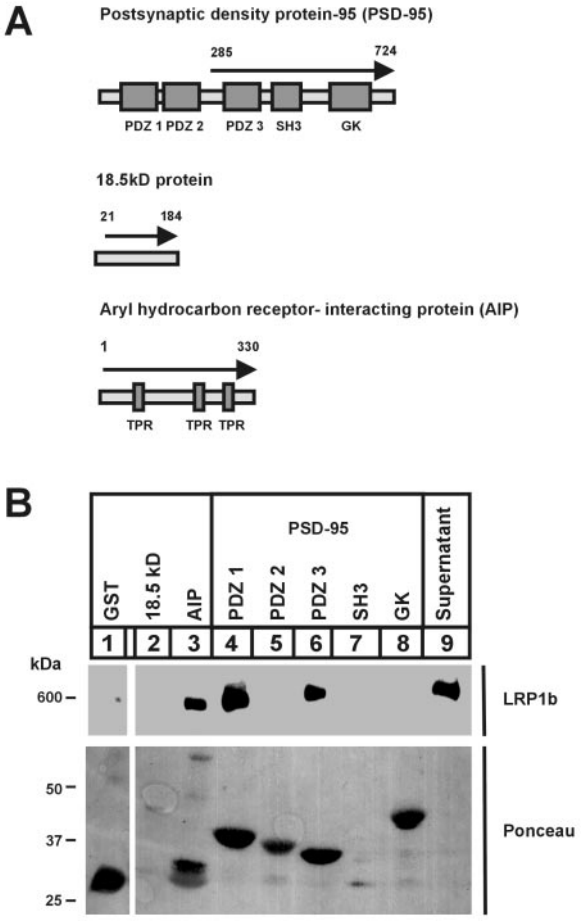

FIG. 8. Intracellular proteins interacting with the cytoplasmic LRP1b tail. (A) The structures of the three interacting proteins identified in the yeast two-hybrid screen are shown. Individual domains of the proteins are shown by dark rectangles. The arrows with numbers indicate the amino acids encoded by the inserts present in the isolated prey vectors. (B) The isolated clones were directly transferred into a GST vector (18.5-kDa protein and AIP) or individual domains were amplified by PCR and cloned into the GST vector (PSD-95). Fusion proteins were bound to glutathione agarorose and incubated with crude membrane preparations (250 μg of brain membranes per sample) from wild-type mouse brain. After washing, the beads were eluted with SDS sample buffer and 9/10 of the eluate was separated by SDS–4% PAGE. The Western blot of the pellet fractions of beads expressing GST alone (lane 1), the 18.5-kDa protein (lane 2), AIP (lane 3), and individual domains of PSD-95 (lanes 4 to 8) with the LRP1b specific antibody is shown. Lane 9 shows LRP1b in the supernatant fraction. The bottom panel shows the Ponceau staining of an SDS gel (4 to 15% acrylamide) loaded with the same samples (1/10 of the pellet fraction).

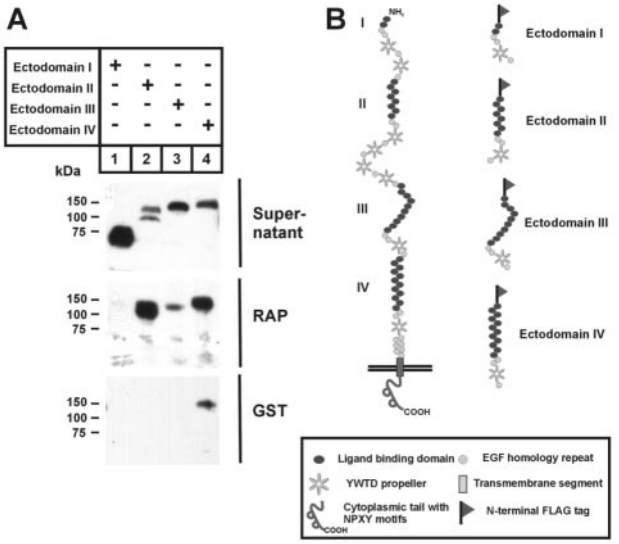

FIG. 9. Expression of LRP1b ectodomains and binding to RAP. (A) HEK 293 cells were transfected with plasmids coding for ectodomains containing the ligand-binding domain region I, II, III, or IV of LRP1b with three amino-terminal FLAG tags. At 48 h after transfection, the supernatants were harvested and loaded directly or after pull-down with GST-RAP or GST on SDS gels (4 to 15% acrylamide). After transfer to nitrocellulose membranes, the ectodomains were detected with a monoclonal anti-FLAG antibody. (B) The structures of the FLAG-tagged LRP1b ectodomains are shown.

DISCUSSION

We have generated LRP1b knockout mice. The absence of the LRP1b protein in these animals was demonstrated by Western blotting. Despite this genetic defect the mice appear phenotypically normal and no functional deficiencies were detected in any of the assays we have performed to date. These findings may be due to functional redundancy among members of the LDL receptor family. The most likely candidate that could compensate for a lack of LRP1b is LRP1. Due to the lethal phenotype of mice lacking LRP1 in the germ line (9), we could not directly answer this question. The approximately 20% of LRP1 expression in RAP$^{-/-}$ mice appears to be enough to compensate for the lack of LRP1b, since LRP1b$^{-/-}$; RAP$^{-/-}$ mice also appeared normal. In contrast to mice lacking the VLDL receptor or ApoER2 (30), no deficits in LTP were observed in LRP1b$^{-/-}$ or LRP1b$^{-/-}$; RAP$^{-/-}$ mice. In addition, we did not find an upregulation of the LRP1 protein in LRP1b$^{-/-}$ animals (Fig. 2C). At this point, we thus cannot rule out the possibility that other receptors of the LDL receptor family or unrelated proteins may compensate for the absence of the receptor in the LRP1b$^{-/-}$ mice.

In the first report of LRP1b a broad distribution of the receptor in human tissues, similar to LRP1, was reported (19). However, in a subsequent publication, LRP1b was found to be largely confined to the brain (18). Using RT-PCR we found LRP1b to be expressed in mouse brain, adrenal gland, and testis. In all other tissues tested, including liver, lung, kidney, muscle, adipose tissue, and the digestive tract, no LRP1b specific transcripts could be detected with this highly sensitive method. The expression of LRP1b in the testis appears to be quite low, since the receptor could not be detected in this tissue by two other methods (Western blot and in situ hybridization). In addition, normal fertility was observed in male (and female) LRP1b$^{-/-}$ mice. Due to technical problems, the expression of LRP1b in the adrenal gland could not be further investigated by Western blotting or in situ hybridization. The presence of the LRP1b in the dentate gyrus of the hippocampus suggests a possible function in synaptic transmission that may be important for a number of physiological functions, e.g., memory and learning. Yet, synaptic plasticity, as determined by LTP measurements was found to be normal in LRP1b$^{-/-}$ mice.

LRP1b contains two additional exons that are not present in the closely related LRP1. Exon 68 codes for an additional ligand-binding repeat in the fourth ligand-binding domain region. The second one, exon 90, codes for 33 amino acids within the cytoplasmic tail without homologies to other known proteins. Interestingly, we found an alternatively spliced form of LRP1b that lacks exon 90. The shorter LRP1b form is present in brain, adrenal gland and testis, whereas the full-length receptor appears to be expressed exclusively in the brain. It is tempting to speculate that these two variants of LRP1b may serve different functions, possibly by mediating different signaling pathways. A similar alternative splicing event within the cytoplasmic tail is known for ApoER2 (4, 16).

Of the three large LDL receptor family members known, LRP1 is known to be processed by the proteinase furin in a *trans*-Golgi compartment, leading to two noncovalently linked protein chains of 515 and 85 kDa. Megalin, on the other hand, is present as an uncleaved 600-kDa receptor on the cell sur-

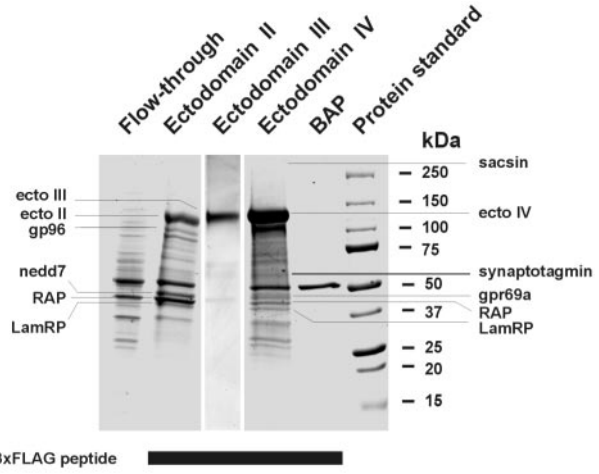

FIG. 10. Affinity purification of brain lysate on LRP1b ectodomains bound to anti-FLAG agarose. FLAG-tagged ectodomains containing the ligand-binding region II, III, and IV of LRP1b were purified from the supernatant of stably transfected 293S cells using anti-FLAG agarose. The immobilized ectodomains and FLAG-tagged BAP as a control were incubated with the same amount of brain lysate overnight and then washed extensively. Bound proteins were eluted with 3xFLAG peptide and separated by SDS-PAGE (4 to 15% acrylamide). The nonbinding fraction (flowthrough) was diluted 1:200 and loaded as a control. Protein bands were visualized with Coomassie (ectodomains II and IV) or silver staining (ectodomain III). Bands were cut out and analyzed by reversed-phase nano-HPLC–ion-trap mass spectroscopy. Proteins identified in each band by mass spectroscopy are indicated. Ecto, ectodomain; LamRP, laminin receptor precursor.

TABLE 2. Potential extracellular ligands of LRP1b as identified by affinity purification and mass spectroscopy[a]

Protein	Peptide(s)	Expression	Localization	Molecular mass (kDa)	Function(s)	Ecto-domain
Sacsin	DSAPTTPTSPTEFLTPGLR, ILLPDTNLLLLPAK	Broad	?	437	Chaperone (?)	IV
Gp96 (grp94)	EEEAIQLDGLNASQIR, GVVDSDDLPLNVSR, SILFVPTSAPR, SGYLLPDTK, EEASDYLELDTIK	Ubiquitous	ER, secreted	96	Chaperone, antigen presentation	II, III
Synaptotagmin I	VPYSELGGK, NTLNPYYNESFSFEVPFEQIQK	Brain, adrenal gland	Synaptic vesicle	65	Exocytosis (Ca^{2+} sensor)	IV
Nedd7	TIVITSHPGQIVK, QISQAYEVLADSK	?	?	44	DnaJ-class chaperone	II
Gpr69a (LanC-like)	SLAENYFDSTGR	Broad	Membrane	40	?	IV
RAP	IQEYNVLLDTLSR, HVESIGDPEHISR, LIHNLNVILAR, VSHQGYGSTTEFEEPR	Ubiquitous	ER	39	Chaperone	II, IV
Laminin receptor precursor (MGr1-Ag)	AIVAIENPADVSVISSR	Broad	Secreted	37	Adhesion, prion protein receptor	II, IV

[a] Potential extracellular ligands are listed with the peptide sequences identified by reversed-phase nano-HPLC–ion trap mass spectroscopy. In addition, the expression pattern, subcellular localization, molecular mass, and presumed function of the proteins are listed. Ectodomains used for the purification of the respective proteins are indicated. ?, unknown.

face. Liu et al. have reported that an LRP1b minireceptor comprising the fourth ligand-binding domain cluster is also cleaved by furin in CHO cells (18). In contrast to this report, we consistently observed only a single band at approximately 600 kDa in our Western blots of endogenous LRP1b. We were also unable to detect a lower molecular-weight band in HEK 293 cells transfected with two independently cloned minireceptor constructs similar to the one reported by Liu et al. The discrepancy between these findings may be explained by individual characteristics of the cell lines used by Liu et al. and in our experiments. However, the absence of a band at the expected molecular size of approximately 85 kDa in Western Blots of endogenous mouse brain LRP1b strongly suggests that LRP1b, like megalin, is present in a single chain form on the cell surface in vivo. In the correctly folded receptor, the furin consensus sequence (REKR, amino acids 3954 to 3957) of LRP1b may not be accessible to the protease. Similarly, rat (but not human) megalin contains a potential furin cleavage site in the absence of evidence for a furin-mediated cleavage event (24).

Several members of the LDL receptor gene family fulfill important functions in cellular signaling pathways. The VLDL receptor and the ApoER2 have been identified as receptors for the signaling protein reelin and thereby control the migration of neurons in the developing brain (29). LRP1, the closest relative of LRP1b, forms a complex with the PDGF receptor β and plays an important role in protecting vascular wall integrity by controlling PDGF receptor activation (3). Previously, a number of intracellular signaling and adaptor molecules that bind to the cytoplasmic domains of LDL receptor family members have been identified (7). Since LRP1b has one of the longest cytoplasmic tails of all LDL receptor family members, it is likely to be involved in intracellular signaling events. Using a yeast two-hybrid screen, three intracellular proteins binding to the LRP1b tail were identified. For two of those, PSD-95 and AIP, the binding to LRP1b could be independently verified in a GST pulldown assay. We were able to map the binding site to the first and third PDZ domain of PSD-95. The interaction of LRP1b with PSD-95 could thus serve to cluster the receptor, e.g., to NMDA receptors, which are known to bind to the first two PDZ domains of PSD-95 via their NR2 subunits (26). Since other family members (LRP1 and ApoER2) are also expressed in neurons and bind to PSD-95, they might compensate for the absence of LRP1b in the LRP1b$^{-/-}$ mice.

The AhR is a xenobiotic receptor that is known to transcriptionally activate cytochrome P450 enzymes (CYP 1A1 and CYP 1A2) after nuclear translocation and heterodimerization with AhR nuclear translocator (ARNT, also known as HIF-1β). AIP, which is also referred to as XAP2 and ARA9, contains three TPR and is part of the unliganded cytosolic AhR complex. AIP has been shown to modify the transcriptional activity of AhR by different mechanisms, including stabilization of the unliganded cytoplasmic AhR and modulating its subcellular localization (reviewed in 22). By interacting with the AIP, LRP1b could modify the response of AhR to its ligands, which include the carcinogen 2,3,7,8 tetrachlorodibenzo-*p*-dioxin (TCDD). This may be of relevance to the function of LRP1b as a tumor suppressor, which was postulated in the first report of this receptor. Interestingly, another intracellular protein (MegBP) containing two TPR has recently been reported to bind to the cytoplasmic tail of megalin (21).

Using affinity purification on LRP1b ectodomains bound to agarose beads, we were able to identify six previously unknown potential extracellular binding partners of LRP1b. The presence of RAP, a known binding partner of LDL receptor family members and previously shown to bind to LRP1b (18) (Fig. 9), within the identified bands provides an internal control for the feasibility of this approach. Most of the bands from which these binding proteins were identified appear to be enriched with respect to the unbound fraction (flowthrough) and are therefore unlikely to be contaminating abundant proteins. This point is stressed by the fact that no bands were observed in the eluate from the control column (BAP). Most of the newly identified ligands are well-known or postulated molecular chaperones. This result highlights the role of folding chaperones in the secretion of LDL receptor family members with their highly complex tertiary structure (12). Some of the newly identified ligands of LRP1b are of particular interest with respect to possible physiological functions of the receptor. Sacsin is a large putative chaperone for which two mutations leading to a truncated protein have been described in patients suffering from autosomal recessive spastic ataxia of Charlevoix-Saguenay (5). Gp96 (also known as grp94) is an endoplasmic reticulum-resident chaperone that is released in a complex

with antigenic peptides from necrotic cells. Interestingly, the homologous LRP1 has been identified as a receptor for gp96 leading to the presentation of the antigenic peptides on major histocompatibility complex class I molecules (2). It remains to be determined whether LRP1b is expressed on antigen-presenting cells and could also play a role in this process. Synaptotagmin I is present in synaptic vesicles and appears to function as a Ca^{2+} sensor in exocytosis (28). The neuronal cell expressed, developmentally down-regulated gene 7 (nedd7) is a putative DnaJ-class molecular chaperone that has not been characterized further (GI 20830104). GPR69a is a 40-kDa membrane protein with a broad tissue distribution which shows homologies to the lantibiotic synthetase C component (LanC) family of bacterial membrane associated proteins (1). The 37-kDa laminin receptor precursor (also known as the multidrug-resistance-associated protein MGr1-Ag) is a secreted protein which has been proposed as an adhesion molecule that mediates the interaction between endothelial cells and smooth muscle cells (14). In addition, the laminin receptor precursor has been identified to interact with the cellular prion protein (15). As shown in Table 2, most of the newly identified ligands bind to ectodomain II and/or ectodomain IV. This is reminiscent of the binding characteristics of the related LRP1, which also binds most of its ligands through interactions with regions II and IV (13).

Currently, little is known about the physiological function as well as the possible role in tumor formation of LRP1b. Its putative role as a tumor suppressor is challenged by the fact that the receptor is not expressed in most normal tissues, like e.g., normal lung tissue (Fig. 4A). To explain the reported alterations of the LRP1b gene in cells derived from non-small cell lung cancer and urothelial cancer, one would have to assume at least a transient expression of LRP1b during the development of these tumors prior to the inactivation of the receptor. However, the LRP1b$^{-/-}$ mice did not show a higher susceptibility for the development of tumors. It is possible that cofactors like exogenous carcinogens or the concomitant inactivation of other tumor suppressors are necessary to induce tumors in LRP1b$^{-/-}$ mice.

Despite the close structural similarity between LRP1 and LRP1b the physiological role of the latter remains currently unclear. LRP1b most likely arose through a gene duplication from LRP1 and subsequently assumed more-specialized and restricted roles that are likely overlapping to a large extent with those of LRP1. Yet, the high rate at which LRP1b is mutated in frequent forms of human cancers is striking. The molecular understanding of its role there is bound to provide novel insights into the origins of malignant disease in general.

ACKNOWLEDGMENTS

We are indebted to LaMetria Blair for excellent technical assistance and Wen-Ling Niu for valuable advice with some of the experiments. We thank Oliver Bergner for help with the expression of GST fusion proteins and Chris Pomajzl for assistance with the brain histology. Thomas C. Südhof generously provided the PSD-95 plasmid.

P.M. received an Erwin Schroedinger fellowship (J1950-PAT and J2162) from the Austrian FWF. J.B. was supported by the Boehringer Ingelheim Foundation. This study was supported by grants from the NIH (HL20948, HL63762, NS43408), the Alzheimer Association, and the Perot Family Foundation.

REFERENCES

1. **Bauer, H., H. Mayer, A. Marchler-Bauer, U. Salzer, and R. Prohaska.** 2000. Characterization of p40/GPR69A as a peripheral membrane protein related to the lantibiotic synthetase component C. Biochem. Biophys. Res. Commun. **275:**69–74.
2. **Binder, R. J., D. K. Han, and P. K. Srivastava.** 2000. CD91: a receptor for heat shock protein gp96. Nat. Immunol. **1:**151–155.
3. **Boucher, P., M. Gotthardt, W. P. Li, R. G. Anderson, and J. Herz.** 2003. LRP: role in vascular wall integrity and protection from atherosclerosis. Science **300:**329–332.
4. **Brandes, C., S. Novak, W. Stockinger, J. Herz, W. J. Schneider, and J. Nimpf.** 1997. Avian and murine LR8B and human apolipoprotein E receptor 2: differentially spliced products from corresponding genes. Genomics **42:**185–191.
5. **Engert, J. C., P. Berube, J. Mercier, C. Dore, P. Lepage, B. Ge, J. P. Bouchard, J. Mathieu, S. B. Melancon, M. Schalling, E. S. Lander, K. Morgan, T. J. Hudson, and A. Richter.** 2000. ARSACS, a spastic ataxia common in northeastern Quebec, is caused by mutations in a new gene encoding an 11.5-kb ORF. Nat. Genet. **24:**120–125.
6. **Frykman, P. K., M. S. Brown, T. Yamamoto, J. L. Goldstein, and J. Herz.** 1995. Normal plasma lipoproteins and fertility in gene-targeted mice homozygous for a disruption in the gene encoding very low density lipoprotein receptor. Proc. Natl. Acad. Sci. USA **92:**8453–8457.
7. **Gotthardt, M., M. Trommsdorff, M. F. Nevitt, J. Shelton, J. A. Richardson, W. Stockinger, J. Nimpf, and J. Herz.** 2000. Interactions of the low density lipoprotein receptor gene family with cytosolic adaptor and scaffold proteins suggest diverse biological functions in cellular communication and signal transduction. J. Biol. Chem. **275:**25616–25624.
8. **Herz, J., and H. H. Bock.** 2002. Lipoprotein receptors in the nervous system. Annu. Rev. Biochem. **71:**405–434.
9. **Herz, J., D. E. Clouthier, and R. E. Hammer.** 1992. LDL receptor-related protein internalizes and degrades uPA-PAI-1 complexes and is essential for embryo implantation. Cell **71:**411–421.
10. **Herz, J., J. L. Goldstein, D. K. Strickland, Y. K. Ho, and M. S. Brown.** 1991. 39-kDa protein modulates binding of ligands to low density lipoprotein receptor-related protein/alpha 2-macroglobulin receptor. J. Biol. Chem. **266:**21232–21238.
11. **Herz, J., U. Hamann, S. Rogne, O. Myklebost, H. Gausepohl, and K. K. Stanley.** 1988. Surface location and high affinity for calcium of a 500-kd liver membrane protein closely related to the LDL-receptor suggest a physiological role as lipoprotein receptor. EMBO J. **7:**4119–4127.
12. **Herz, J., and P. Marschang.** 2003. Coaxing the LDL receptor family into the fold. Cell **112:**289–292.
13. **Herz, J., and D. K. Strickland.** 2001. LRP: a multifunctional scavenger and signaling receptor. J. Clin. Investig. **108:**779–784.
14. **Hu, C., J. A. Oliver, M. R. Goldberg, and Q. Al Awqati.** 2001. LRP: a new adhesion molecule for endothelial and smooth muscle cells. Am. J. Physiol. Renal Physiol. **281:**F739–F750.
15. **Hundt, C., J. M. Peyrin, S. Haik, S. Gauczynski, C. Leucht, R. Rieger, M. L. Riley, J. P. Deslys, D. Dormont, C. I. Lasmezas, and S. Weiss.** 2001. Identification of interaction domains of the prion protein with its 37-kDa/67-kDa laminin receptor. EMBO J. **20:**5876–5886.
16. **Kim, D. H., K. Magoori, T. R. Inoue, C. C. Mao, H. J. Kim, H. Suzuki, T. Fujita, Y. Endo, S. Saeki, and T. T. Yamamoto.** 1997. Exon/intron organization, chromosome localization, alternative splicing, and transcription units of the human apolipoprotein E receptor 2 gene. J. Biol. Chem. **272:**8498–8504.
17. **Langbein, S., O. Szakacs, M. Wilhelm, F. Sukosd, S. Weber, A. Jauch, B. A. Lopez, P. Alken, T. Kalble, and G. Kovacs.** 2002. Alteration of the LRP1B gene region is associated with high grade of urothelial cancer. Lab Investig. **82:**639–643.
18. **Liu, C. X., Y. Li, L. M. Obermoeller-McCormick, A. L. Schwartz, and G. Bu.** 2001. The putative tumor suppressor LRP1B, a novel member of the low density lipoprotein (LDL) receptor family, exhibits both overlapping and distinct properties with the LDL receptor-related protein. J. Biol. Chem. **276:**28889–28896.
19. **Liu, C. X., S. Musco, N. M. Lisitsina, E. Forgacs, J. D. Minna, and N. A. Lisitsyn.** 2000. LRP-DIT, a putative endocytic receptor gene, is frequently inactivated in non-small cell lung cancer cell lines. Cancer Res. **60:**1961–1967.
20. **Nykjaer, A., and T. E. Willnow.** 2002. The low-density lipoprotein receptor gene family: a cellular Swiss army knife? Trends Cell Biol. **12:**273–280.
21. **Petersen, H. H., J. Hilpert, D. Militz, V. Zandler, C. Jacobsen, A. J. Roebroek, and T. E. Willnow.** 2003. Functional interaction of megalin with the megalinbinding protein (MegBP), a novel tetratrico peptide repeat-containing adaptor molecule. J. Cell Sci. **116:**453–461.
22. **Petrulis, J. R., and G. H. Perdew.** 2002. The role of chaperone proteins in the aryl hydrocarbon receptor core complex. Chem. Biol. Interact. **141:**25–40.
23. **Reeves, P. J., R. L. Thurmond, and H. G. Khorana.** 1996. Structure and function in rhodopsin: high level expression of a synthetic bovine opsin gene

and its mutants in stable mammalian cell lines. Proc. Natl. Acad. Sci. USA **93:**11487–11492.

24. **Saito, A., S. Pietromonaco, A. K. Loo, and M. G. Farquhar.** 1994. Complete cloning and sequencing of rat gp330/"megalin," a distinctive member of the low density lipoprotein receptor gene family. Proc. Natl. Acad. Sci. USA **91:**9725–9729.
25. **Shelton, J. M., M. H. Lee, J. A. Richardson, and S. B. Patel.** 2000. Microsomal triglyceride transfer protein expression during mouse development. J. Lipid Res. **41:**532–537.
26. **Sheng, M., and D. T. Pak.** 1999. Glutamate receptor anchoring proteins and the molecular organization of excitatory synapses. Ann. N. Y. Acad. Sci. **868:**483–493.
27. **Silva, A. J., T. W. Rosahl, P. F. Chapman, Z. Marowitz, E. Friedman, P. W. Frankland, V. Cestari, D. Cioffi, T. C. Sudhof, and R. Bourtchuladze.** 1996. Impaired learning in mice with abnormal short-lived plasticity. Curr. Biol. **6:**1509–1518.
28. **Sudhof, T. C.** 2002. Synaptotagmins: why so many? J. Biol. Chem. **277:**7629–7632.
29. **Trommsdorff, M., M. Gotthardt, T. Hiesberger, J. Shelton, W. Stockinger, J. Nimpf, R. E. Hammer, J. A. Richardson, and J. Herz.** 1999. Reeler/Disabled-like disruption of neuronal migration in knockout mice lacking the VLDL receptor and ApoE receptor 2. Cell **97:**689–701.
30. **Weeber, E. J., U. Beffert, C. Jones, J. M. Christian, E. Forster, J. D. Sweatt, and J. Herz.** 2002. Reelin and ApoE receptors cooperate to enhance hippocampal synaptic plasticity and learning. J. Biol. Chem. **277:**39944–39952.
31. **Willnow, T. E., S. A. Armstrong, R. E. Hammer, and J. Herz.** 1995. Functional expression of low density lipoprotein receptor-related protein is controlled by receptor-associated protein in vivo. Proc. Natl. Acad. Sci. USA **92:**4537–4541.
32. **Willnow, T. E., and J. Herz.** 1994. Homologous recombination for gene replacement in mouse cell lines. Methods Cell Biol. **43:**305–334.
33. **Willnow, T. E., J. Hilpert, S. A. Armstrong, A. Rohlmann, R. E. Hammer, D. K. Burns, and J. Herz.** 1996. Defective forebrain development in mice lacking gp330/megalin. Proc. Natl. Acad. Sci. USA **93:**8460–8464.
34. **Willnow, T. E., J. M. Moehring, N. M. Inocencio, T. J. Moehring, and J. Herz.** 1996. The low-density-lipoprotein receptor-related protein (LRP) is processed by furin in vivo and in vitro. Biochem. J. **313:**71–76.
35. **Willnow, T. E., K. Orth, and J. Herz.** 1994. Molecular dissection of ligand binding sites on the low density lipoprotein receptor-related protein. J. Biol. Chem. **269:**15827–15832.
36. **Wu, L. G., and P. Saggau.** 1994. Presynaptic calcium is increased during normal synaptic transmission and paired-pulse facilitation, but not in long-term potentiation in area CA1 of hippocampus. J. Neurosci. **14:**645–654.